Zoomorphology (2023) 142:377–392
https://doi.org/10.1007/s00435-023-00602-x

ORIGINAL PAPER

Extraembryonic membrane morphology in greater rheas (*Rhea americana americana* Linnaeus, 1758)

Ana Indira Bezerra Barros Gadelha[1,2,3] · Moacir Franco de Oliveira[1] · Ana Caroline Freitas Caetano de Sousa[2] · João Augusto Rodrigues Alves Diniz[1,2,4] · Igor Renno Guimarães Lopes[1,2,4] · Bruno Caio Chaves Fernandes[5] · Alexsandra Fernandes Pereira[1] · Carlos Eduardo Bezerra de Moura[1]

Received: 21 December 2022 / Revised: 16 January 2023 / Accepted: 27 February 2023 / Published online: 20 March 2023

Abstract

The greater rhea, *Rhea americana*, is a wild ratite of high scientific importance and significant and zootechnical value, especially considering the current development state of Brazilian poultry production, where research aimed at increasing the productivity of these animals has become extremely relevant. Studies concerning fetal attachments and embryonic development are paramount, as they can provide essential information concerning reproductive and nutritional animal management. However, a lack of information on greater rhea fetal morphology is noted. Therefore, the aim of the present study was to establish a standard model for fetal attachments in this species. Greater rhea eggs were incubated from 0 to 36 days, and macroscopic and microscopic embryonic attachment characterizations were performed. Histologically, all embryonic annexes exhibit germ layers, namely the ectoderm (outer layer), mesoderm (middle layer) and endoderm (inner layer). The findings indicate that greater rhea development patterns are similar to other birds.

Keywords Fetal attachments · Germ layers · Morphology · Ratites

Introduction

The greater rhea (*Rhea americana americana*) is a ratite belonging to the Rheidae family and *Rhea* genus (Sousa et al. 2018). This species is distributed throughout different Brazilian regions, i.e., the midwest, south and northeast (Sick 2001), displaying scientific importance due to its captivity adaptability (Costa et al. 2018) and zootechnical value, due to the high amount of greater rhea by-products, such as meat, eggs, leather, feathers and oil (Romanelli et al. 2008; Torquato et al. 2015). Considering the marked development of the Brazilian poultry sector in recent years, research aimed to further knowledge on avian reproductive and productive periods are relevant to avoid losses during embryonic development, offering better management conditions (Groff et al. 2017).

According to Thierry et al. (2013), animal embryonic development assessments promote access to essential information, allowing for the identification of potential food management problems and behavioral changes during egg incubation periods, also aiding in identifying issues associated with environmental conditions, hormonal changes and alterations arising from stress, as highlighted by Ouyang et al. (2012).

Extraembryonic membranes promote embryonic development, providing nutrition, excretion, and gas exchange conditions, as well as protection and support for developing embryos (Mess 2003). Because of this and their easy availability, avian fetal membranes have been employed as pharmaceutical models (Vargas et al. 2007), in embryology,

✉ Ana Indira Bezerra Barros Gadelha
anaindirabezerra@hotmail.com

1 Postgraduate Program in Animal Science, Federal Rural University of Semi-Árido, Rio Grande do Norte, Mossoró, Brazil

2 Department of Animal Sciences, Federal Rural University of Semi-Árido, Rio Grande do Norte, Mossoró, Brazil

3 Masters Program in Development and Environment, Federal Rural University of Semi-Árido, Rio Grande do Norte, Mossoró, Brazil

4 Doctoral Program in Development and Environment, Federal Rural University of Semi-Árido, Rio Grande do Norte, Mossoró, Brazil

5 Department of Phytotechny, Federal Rural University of Semi-Árido, Rio Grande do Norte, Mossoró, Brazil

morphology, biochemistry, and physiology studies (Narbaitz et al. 1995) and in neoplasm, angiogenesis (Ribatti 2012) and embryotoxicity (Winter et al. 2013) assessments. The literature also reports the use of extraembryonic avian attachments in research associated to hematopoietic events, healing stimulation, virus isolation and identification, stem cell production, proteomics, and cell therapy (Gadelha et al. 2021).

In this context, this study aimed to describe fetal greater rhea extraembryonic membrane morphology in view of a wide range of research previously carried out using smaller birds as clinical and scientific models and as a way to obtain novel data on species development. This also allows for data on artificial incubation and captive production, as well in attempts to establish a standard model for the fetal membranes of this species, producing subsidies for anatomo-histopathological and embryo diagnoses of clinical interest.

Materials and methods

Sampling

Extraembryonic greater rhea membrane evaluations were carried out at the Center for the Multiplication of Wild Animals (CEMAS) belonging to the Federal Rural University of the Semi-Arid (UFERSA), located in Mossoró, RN, in the semiarid Brazilian Northeastern region (IBAMA No. 14.78912).

Fragments of greater rhea chorion, allantois, yolk sac and amnion were sampled from three eggs belonging to each incubation range (0–24 days), samples 3 days apart (3, 6, 9, 12, 15, 18, 21, 24 days of incubation), with one egg analyzed from 27 to 36 days of incubation (27, 30, 33, 36), totaling 28 eggs. Embryonic attachments were described both macro- and microscopically.

The eggs were collected early in the morning, sanitized, and maintained in an Luna 240/Chocmaster incubator (Premium Ecológica Ltda.), arranged horizontally at an average temperature of ± 36.5 °C and relative humidity of 52–56%, considering the 24-h interval as the first day of the incubation process.

For the extraembryonic membrane development descriptions, the eggs were opened by means of a microgrinder (DREMEL 3000), positioned in the pole of the air chamber, followed by insertion of a cotton swab soaked with an overdose of isofluorane (Isoforine®, Cristália Produtos Químicos Farmacêutico Ltda). The eggs were then wrapped in a PVC film (Wyda®, Alukenti Embalagens Ltda) containing the anesthetic to ensure analgesia and death within 10 min. Embryos at less than 10 days of incubation were euthanized by hypothermia, maintained below 4 °C for up to one hour (Federal Council of Veterinary Medicine, CFMV, 2013).

Bioethics

This study was approved and performed under UFERSA Committee on Ethics and Welfare in the Use of Animals guidelines (CEUA, nº 32/ 2020) and authorized by the Instituto Chico Mendes de Biodiversidade (ICMBio, nº 75,369).

Macro- and microscopic fetal rhea attachment characterizations

All embryos and structures were first macroscopically analyzed. For the subsequent microscopic analyses, embryos and structures were fragmented into small pieces for better fixative absorption and soaking (in paraformaldehyde, glutaraldehyde and karnovsky solutions) according to the applied procedure (light microscopy, scanning microscopy or transmission microscopy, respectively. To this end, three 3-day intervals were considered (3, 6, 9, 12, 15, 18, 21, 24, 27, 30, 33, and 36 days of incubation), for external morphology assessments during different embryonic and fetal development stages (Almeida et al. 2015), all surfaces were analyzed (ventral, medial, lateral and dorsal) with a magnifying glass (ESTEK), and the structures were photographed, schematized and named according to the Handbook of Aviantomy: Nomina Anatomic Avium (1993). All data were compared to the relevant literature. The opened eggs were immersed in water to allow for structure movement and analysis without damage.

Light microscopy analyses

Embryo and structure fragments were fixed in PBS-buffered 4% paraformaldehyde for 72 h and subsequently dehydrated in an increasing ethanol series (70%, 90%, 95%, 90%, 95%, 100% and 100%) for 30 min at each concentration and placed in two Xylol baths for 30 min. The fragments were then paraffinized with histological paraffin (Bandeirante Química Ltda) (two baths, one for 6 h and the other for 1 h) and then embedded in paraffin. Finally, 5 µm-thick sections were obtained, placed on glass slides, and left in a drying oven at 60 °C for 4 h, for subsequent staining in hematoxylin and eosin (HE) according to Tolosa et al. (2003). The slides were analyzed under a Leica ICC50 HD light microscope and images were obtained using the LAS EZ Ink software.

Scanning electron microscopy (SEM) analyses

Fragments of the yolk sac, chorion, allantois, and amnion of eggs at 12, 18, and 24 days of incubation and the shell + chorioallantois at 39 days after oviposition were used for the

SEM analyses, only these two membranes were collected after the animals' oviposition, as they remained present and aggregated in the egg even after the animals' birth. This was done to verify their complexity without interventions in animals' incubation or birth. The fragments were fixed in 2.5% glutaraldehyde buffered with 0.1 M PBS and pH 7.4, washed with PBS buffer, post-fixed with 1% osmium tetroxide buffered with 0.1 M PBS and pH 7.4 from 30 min to 1 h and washed with distilled water (three baths of 10 min each). They were then dehydrated in an increasing ethanol series (50%, 70%, 90% and 100%), twice for 15 min at each concentration. Finally, drying was performed employing a critical point device using carbon dioxide (QUORUM® K850, England) followed by mounting on supports (stubs) and metallization by gold sputtering for the SEM analyses employing a LEO VP 435-Carl-Zeis equipment (Oberkochen, Germany).

Transmission electron microscopy (TEM) analyses

For the ultrastructural analyses, fragments measuring about 0.5 mm^2 were obtained from the yolk sac, chorion, allantois, and amnion at 18 days of incubation. The samples were obtained at this age due to complete extraembryonic annexes as verified by macro- and microscopical (light microscopy and scanning electron microscopy) assessments, in excellent condition for this analysis. The fragments were fixed in 2.5% glutaraldehyde buffered with 0.1 M PBS and pH 7.4 for 72 h, washed three times in PBS buffer for 10 min and post-fixed in PBS-buffered osmium tetroxide for 2 h. They were subsequently washed three times with 0.1 a M PBS buffer solution at pH 7.4 for 10 min followed by distilled water for 15 min and dehydration by immersion in an increasing ethanol series (50%, 70%, 80%, 90% and 100%, with three changes every 15 min). Then, each sample was bathed in propylene oxide for 10 min, immersed in a mixture of propylene oxide and Spurr resin in a 1:1 ratio for 1 h and 1:3 for an hour and a half and then immersed in pure Spurr resin for 12 h and included in pure resin to obtain sample blocks, maintained in an oven at 60 °C for 72 h. Subsequently, 0.4 µm-thick semi-thin sections were obtained for material selection and 0.07 µm ultra-thin sections were stained with 2% uranyl acetate and 0.5% lead citrate for analysis under a transmission electron microscope (FEI Company, Netherlands) coupled to a Mega View III Camera (Solf Imaging, Germany).

Results

Macroscopic greater rhea embryo and structure aspects

The embryonic development stages investigated herein indicate a marked dynamism between the four analyzed extraembryonic membranes, including in relation to the shell membrane during incubation progression. The first fetal membrane, the yolk sac, was formed at 3 days of incubation (Fig. 1A). This small circular structure displays peripheral vascular formations originating from the embryo, represented by a vein and an artery that follow until the periphery of the sinus terminalis and branch out to form a vascular area covering the embryo. The amnion, a thin translucent structure in the form of an avascular pouch surrounding the embryo, was also observed at this stage.

At 6 days of incubation (Fig. 1B), the yolk sac exhibits increased vascularization and four large blood vessels emerge from the embryo. The amnion displays greater expansion and vascularization, apparently due to interaction with the allantois, which forms a vascular disc, arranged at the upper pole of the bud.

At 9 days of incubation (Fig. 1C), extraembryonic membrane vascularization originates from an evagination that projects from the urachus, represented by the allantoid diverticulum, which gives rise to two large vessels during its development, which gradually ramify and vascularize the amnion and yolk sac. The amnion is highly vascularized at this stage, with a noticeable presence of fluid forming a pouch where the embryo is immersed in. The presence of the chorion is noticeable at this stage, comprising a thin and translucent layer already in contact with the allantois, although this was only verified after structure manipulation.

On the 12th day of incubation (Fig. 1D), the amnion expands but the amniotic fluid volume is apparently lower, as the membrane maintains a direct relationship with the developing embryo compared to the previous stages. The allantois, is therefore, significantly expanded and its vessels become of a higher caliber and intensely branched, allowing for differentiation between arteries and veins. At this age, an interaction between the allantois and the chorion is also evident, forming the chorioallantoid membrane. Large contact areas between all fetal membranes are observed, with the allantois playing the most significant role, given its many vessels, even when compared to the yolk sac, which is simply a yolk storage structure. On the 15th day of incubation (Fig. 1E), the umbilical allantoid vessels are larger and display increasing ramifications, easily differentiating them from other membranes.

At 18 days of development (Fig. 1F), a significant increase in embryo size and in the amount of amniotic

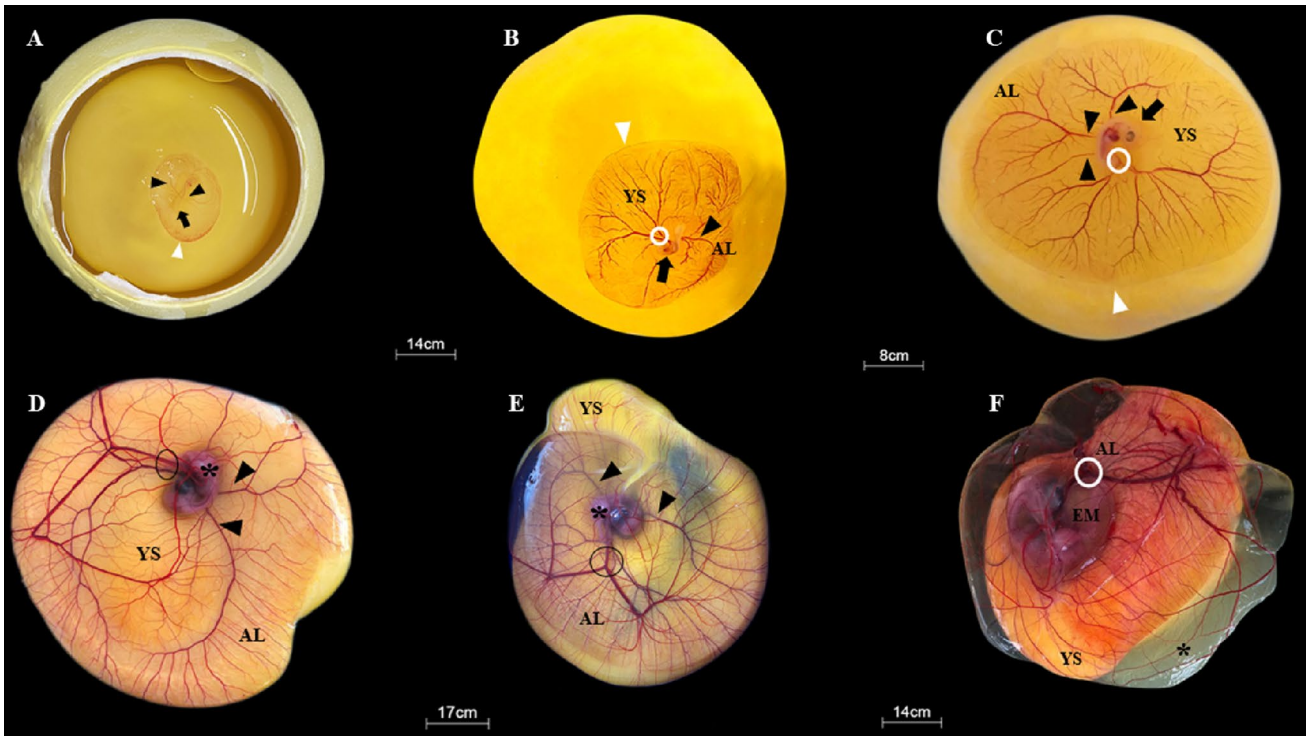

Fig. 1 Greater rhea embryonic attachments. **A** 3 days of incubation. **B** 6 days of incubation. **C** 9 days of incubation. **D** 12th day of incubation. **E** 15th day of incubation. **F** 18th day of incubation. Photo **A**: black arrowhead: vitelline right omphalomesenteric and left omphalomesenteric arteries, black arrow: amnion, white arrowhead: sinus terminalis. Photo **B**: black arrowhead: left omphalomesenteric artery, circle: right omphalomesenteric artery, black arrow: amnion, *YS* yolk sac area, *AL* allantoic area, white arrowhead: sinus terminalis. Photo **C**: black arrowhead: omphalomesenteric arteries, circle: urachus, *AL* allantoic area, *YS* yolk sac area, white arrowhead: sinus terminalis. Photo **D**: black arrowhead: omphalomesenteric arteries, circle: urachus, *YS* yolk sac area, *AL* allantoic area, *black: embryo. Photo **E**: black arrowhead: omphalomesenteric arteries, circle: urachus, *YS* yolk sac area, *AL* allantoic area, *black: embryo. Photo **F**: Circle: urachus, *EM* embryo, *AL* allantoic area, *YS* yolk sac area, *black: albumen. Bars: 14 cm, 5 cm, 9 cm, 17 cm, 14 cm and 15 cm

fluid is noted. A vascular connection between the amnion, allantois and yolk sac is noted dorsal to the embryo. A greater supply of amniotic vessels is noted at this stage to ensure effective embryo-medium exchanges. The allantoid vascular network becomes more branched and developed, vascularizing the yolk sac, also involving the albumen as a way of increasing surface exchange areas. The vitelline vessels that surround the entire yolk mass begin emitting a circular network of vessels. The allantoid vessels are arranged under the yolk mass by juxtaposition. At this stage, the allantois appears to display its maximum development, as it also connected directly to the amnion in its upper portion.

At 21 days of incubation (Fig. 2G), the yolk sac is richly vascularized, almost completely superimposed by the allantois, and its wrinkled appearance indicates yolk absorption. At this stage, the chorioallantoid membrane is in close contact with the shell membrane, suggesting gas and mineral transport from the shell.

At 24 days (Fig. 2H), the allantoid and vitelline vessels are quite turgid, and their network organization suggests that they function as yolk mass traction structures to the interior of the coelomic cavity, retracting throughout the incubation process. At this age, four vessels are evident from the urachus, two arteries and two veins, one larger, which moves laterally when in contact with the yolk mass, branching out over it and emitting small caliber vessels under a very thin membrane containing the yolk.

On the 27th day of incubation (Fig. 2I), the chorionic membrane, previously transparent, becomes easily observed, relatively white as a result of complete allantois interrelation. At this stage, a high concentration of uric acid deposits is noted when compared to previous phases. The yolk sac becomes more reduced due to the yolk absorption process.

On the 30th day of incubation (Fig. 2J), the vitelline arteries and veins move to the left of the fetus, becoming even larger, moving together until they become inserted into the yolk mass, and then becoming small caliber vessels arranged

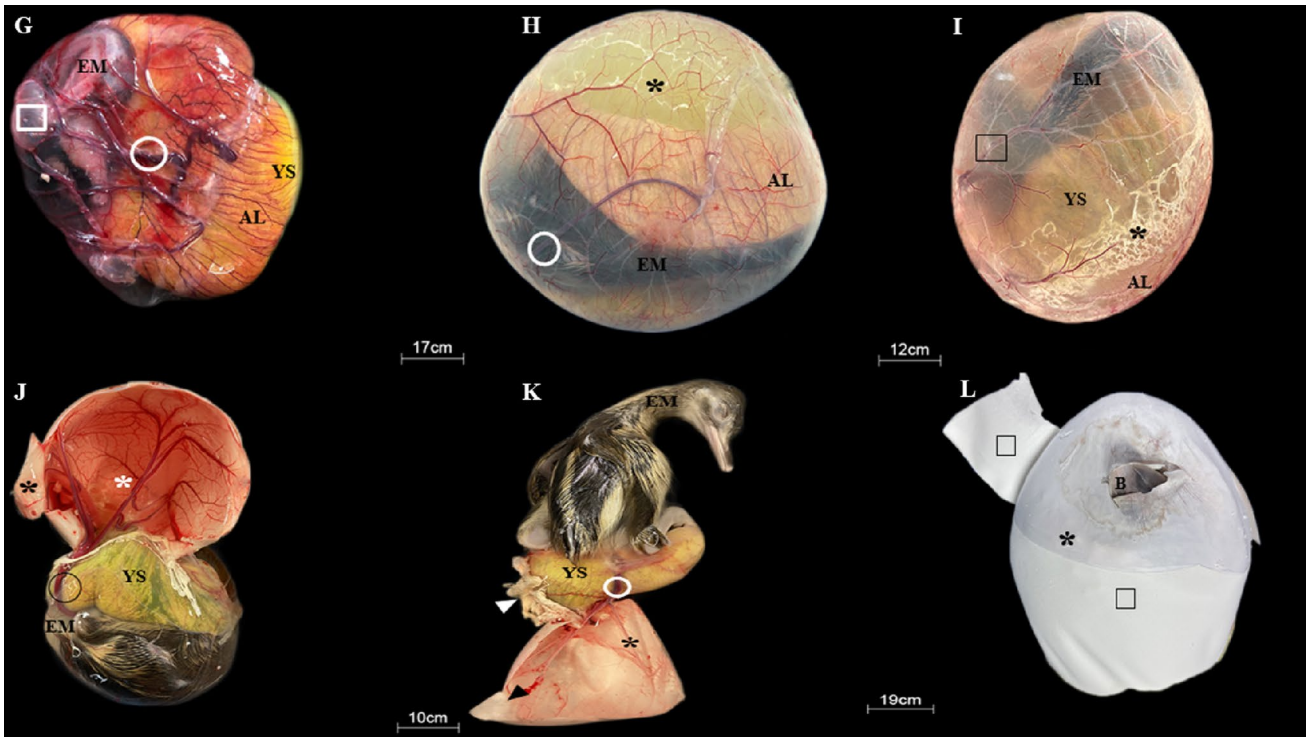

Fig. 2 Greater rhea embryonic attachments. **G** 21st day of incubation. **H** 24th day of incubation. **I** 27th day of incubation. **J** 30th day of incubation. **K** 33rd day of incubation. **L** 36th day of incubation. Photo **G**: white circle: urachus, white square: bubble to indicate another layer under the other attachments, namely the chorion, *AL* allantoic area, *YS* yolk sac area, *EM*: embryo. Photo **H**: white circle: vessels coming from the urachus, *AL* allantoic area, *black: yolk from yolk sac to be absorbed, *EM* embryo. Photo **I**: black square: illustrating that there is a membrane covering the other appendages, the corium, *AL* allantoic area, *black: uric acid, *YS* yolk sac area, *EM* embryo. Photo **J**: *EM* embryo, black circle: urachus, *YS* yolk sac area, *white: area of contact between chorion + allantois and shell membrane, *black: shell membrane. Photo **K**: *EM* embryo, circle: urachus, *YS* yolk sac, white arrowhead: uric acid, black arrowhead: shell membrane, *black: area of contact between the chorion, allantois, and shell membrane. **L**: *black: chorion, *black square: shell membrane, B: greater rhea beak. Bars: 17 cm, 12 cm, 10 cm, 10 cm, 19 cm, 10 cm

in a circular shape. The chorioallantoid membrane reaches its maximum shell membrane adhesion degree at this stage.

Finally, on the 33rd day of incubation (Fig. 2K), a high adhesion to the allantoid vessels is noted under the vitelline membrane, in close association with the chorioallantoid membrane. The arteries and veins become slightly contorted. At 36 days of incubation (Fig. 2L), the embryo has already perforated the membrane complex represented by the chorioallantoid membrane and the shell membrane at the air chamber region. After removing these structures, the yolk sac was identified as completely absorbed. It is noteworthy that rheas may hatch between 36 and 42 days of incubation, depending on the hatchery or ambient temperature.

Fetal attachment microscopy analyses

Yolk sac

The light microscopy analyses (Fig. 3A) indicated the presence of germinative cells in the yolk sac, squamous cells in the ectoderm and large and prismatic cells in the endoderm, as well as erythrocytes. The SEM analyses verified the presence of rounded endodermal cells (Fig. 3B) and the TEM analyses, the presence of both endodermal and ectodermal cells, as well as delimiting cell boundaries (Fig. 3C) and a myelin figure (Fig. 3D) in which the nucleus occupies almost the entire cytoplasmic volume. The endoplasmic reticulum in the yolk sac is well developed and rough (Fig. 3E) and the cytoplasm contains numerous lipid droplets of varying size with a vesicular aspect very similar to that of cytoplasmic organelles (Fig. 3F).

Amnion

Histologically, the amnion is represented by the three embryonic layers, namely the ectoderm, mesoderm, and endoderm. The ectoderm is made up of a stratified epithelium composed of cubic cells, while the endoderm is made up of a squamous epithelium comprising a double layer of cubic cells and the mesoderm, of loose connective tissue. Blood vessels are also observed in the latter (Fig. 4A). The SEM analyses indicated polygonal epidermal cells interspersed with numerous blood

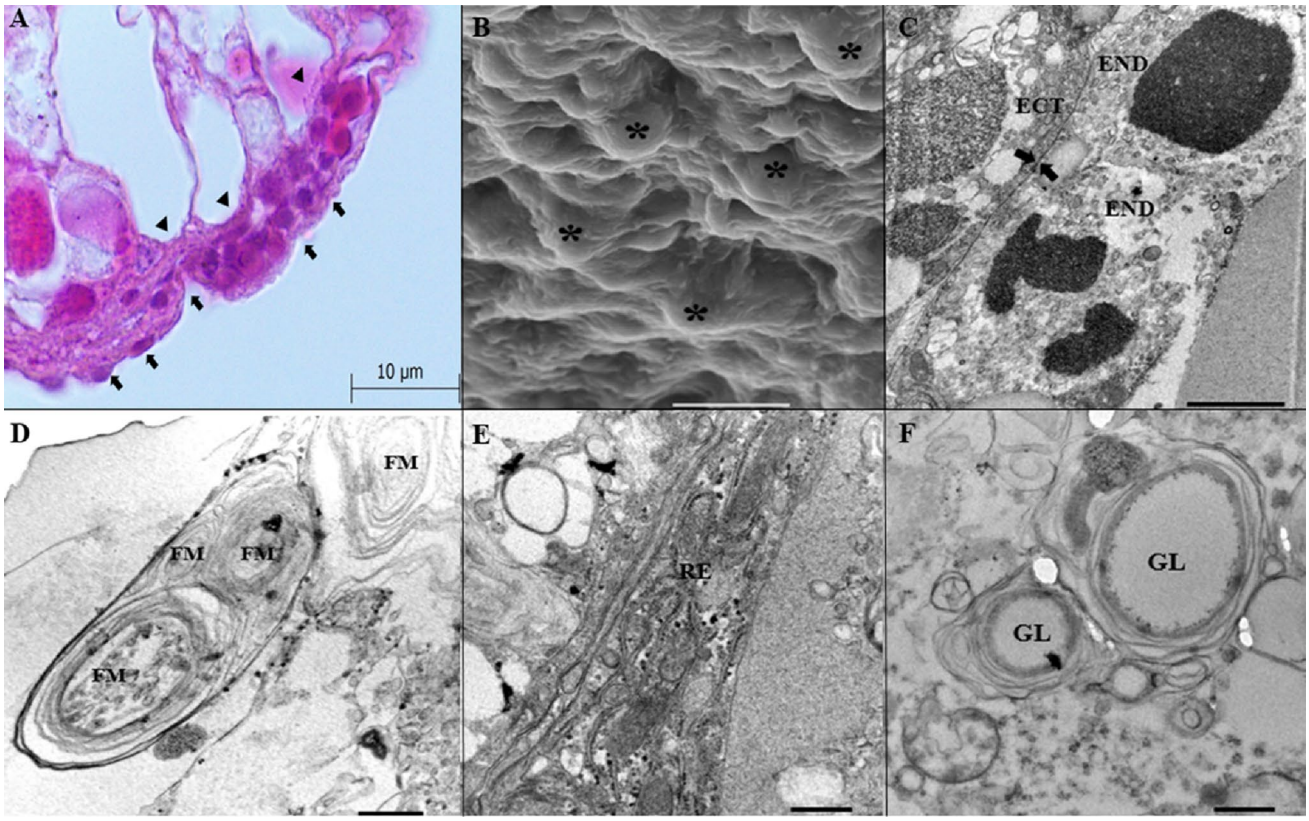

Fig. 3 Greater rhea yolk sac. **A** Yolk sac under light microscopy at 12 days of incubation, **B** yolk sac under scanning electron microscopy at 12 days of incubation; **C**, **D**, **E** and **F** yolk sac under transmission electron microscopy at 18 days of incubation. **A**: black arrow: ectoderm, black arrowhead: endoderm. **B**: *endodermal cells. **C**: arrows (cell boundaries), *ECT* ectodermal cell, *END* endodermal cells. **D**: FM (myelin figure). **E**: ER (rough endoplasmic reticulum). **F**: GL (lipid droplets). Bar: 10 µm, 20 µm, 2 µm, 500 nm, 500 nm, 500 nm

vessels (Fig. 4B, C). The TEM analyses of greater rhea amnion at 18 days of embryonic development indicated an amniotic ectoderm containing fibroblast cells with elongated nuclei (Fig. 4D) and the presence of microfilaments in the mesoderm (Fig. 4E). The cytoplasmic membrane exhibits projections, suggesting transport activities, given the presence of lipid vesicles and small electron-dense vesicles observed at the edge of the endoderm (Fig. 4F).

Allantoid

The allantois of greater rheas at all analyzed stages, similarly to the amnion, is represented by three germ layers, the ectoderm, mesoderm and endoderm. The ectoderm is formed by multiple layers of cubic cells, the mesoderm, of loose connective tissue interposed with blood vessels, and the endoderm, of simple squamous cells containing intercellular spaces at all stages (Fig. 5A). The SEM assessments indicated venules and arteries in the allantois at 12 days of incubation, in addition to a capillary plexus presenting different vascular densities between the intervessel orifices (Fig. 5B). At 24 days of incubation, the endodermal cells exhibit a pyramidal shape (Fig. 5C). The TEM investigation of greater rhea allantois at 18 days of incubation indicated fibroblasts (Fig. 5E), many granules suggestive of the presence of glycogen granules (Fig. 5D, E), as well as many blood capillaries, some pericytes between the capillaries (Fig. 5D) and mesenchyme (Fig. 5E). Rough endoplasmic reticulum was also abundant (Fig. 5F).

Chorioallantois + chorion + shell membrane

At 39 days of incubation, the chorioallantoid membrane is completely adhered to the shell membrane, giving it a vascularized appearance. The light microscopy assessment indicated that the chorioallantoid membrane is made up exclusively of collagen fibers. The ectoderm, mesoderm and endoderm are distinguishable in the chorion, with the ectoderm and endoderm formed by a stratified cubic epithelium and the mesoderm represented by loose connective tissue. The presence of blood vessels is noted in the chorionic membrane (Fig. 6A). The allantoid portion of the membrane is made up of a stratified squamous-type epithelium and a

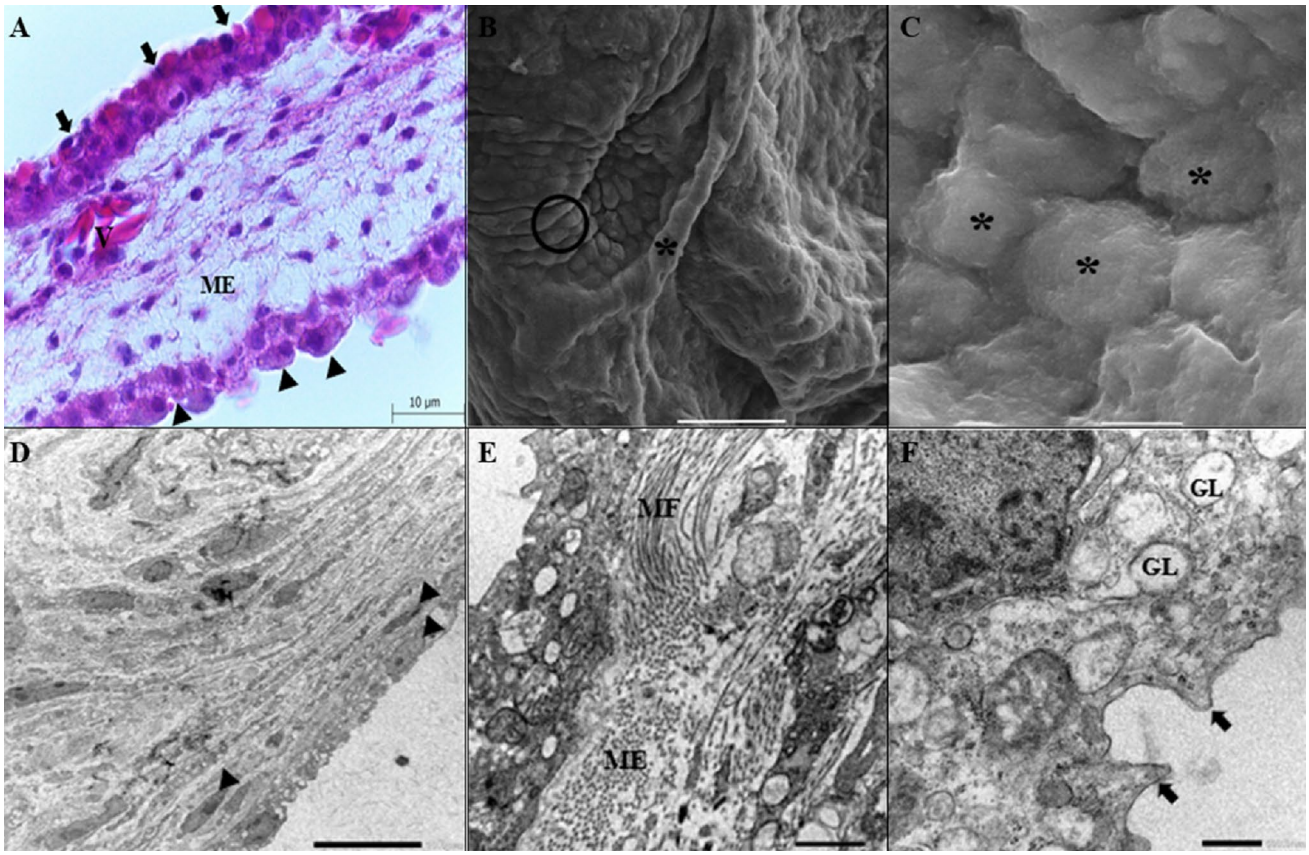

Fig. 4 Greater rhea amnion. **A** Light microscopy amnion at 24 days of incubation, black arrow: ectoderm, black arrowhead: endoderm, V: blood vessels, ME: mesoderm. **B** Scanning electron microscopy at 24 days of incubation, *blood vessel, circle (villi). **C** Scanning electron microscopy at 18 days of incubation, *(epithelial cells). **D** Transmission electron microscopy at 18 days of incubation, arrowhead: fibroblasts. **E** Transmission electron microscopy at 18 days of incubation, *MF* microfilaments, *ME* mesoderm. **F** Transmission electron microscopy at 18 days of incubation, *GL* lipid droplets, arrows: microvilli. Bar: 10 µm, 50 µm, 5 µm, 10 µm, 1 µm, 500 nm

layer of loose conjunctiva nature still connects the two membranes. The presence of many blood vessels is noted.

The SEM investigation demonstrated collagen fibers and calcium deposits in the shell membrane (Fig. 6B). At 27 days of incubation, the chorioallantoid membrane contains blood vessels and the shell membrane, parallel fibers (Fig. 6C). The fragments of the chorioallantoid membrane alongside the shell membrane at 39 days of incubation contain numerous oval cells in the subepithelial chorion layer, whereas numerous elongated epithelial cells are observed in the subepithelial layer of the allantois. Blood vessels and fibroblast-like cells make up the connective mesoderm tissue (Fig. 6D). The TEM assessment indicated that the chorion when analyzed separately contains blood capillaries, blood vessels, pericytes, basal cells (Fig. 6E) and epithelial trabeculae (Fig. 6F).

Discussion

Macroscopical fetal attachment assessments

Greater rhea fetal membranes, comprising the amnion, allantoid, chorion and yolk sac, display a development pattern where the yolk sac becomes visible in the first 3 days of incubation, followed by the amnion at 6 days and the allantoid at 9 days. An interaction with the chorioallantoid membrane begins at 12 days of incubation, and at 36 days, the yolk sac is almost completely absorbed, noting that at this date the chick has already perforated the shell membrane. The appearance of extraembryonic membranes in this order seems to be associated with their functions during the embryonic process, such as the presence of the yolk sac visualized before the amnion indicating that, although birds require the amnion as a membrane that delimits a water reservoir to develop in non-aquatic environments, they first require a nutrient reservoir, similarly to other animals. Thus, the yolk sac is visualized before other appendages due to

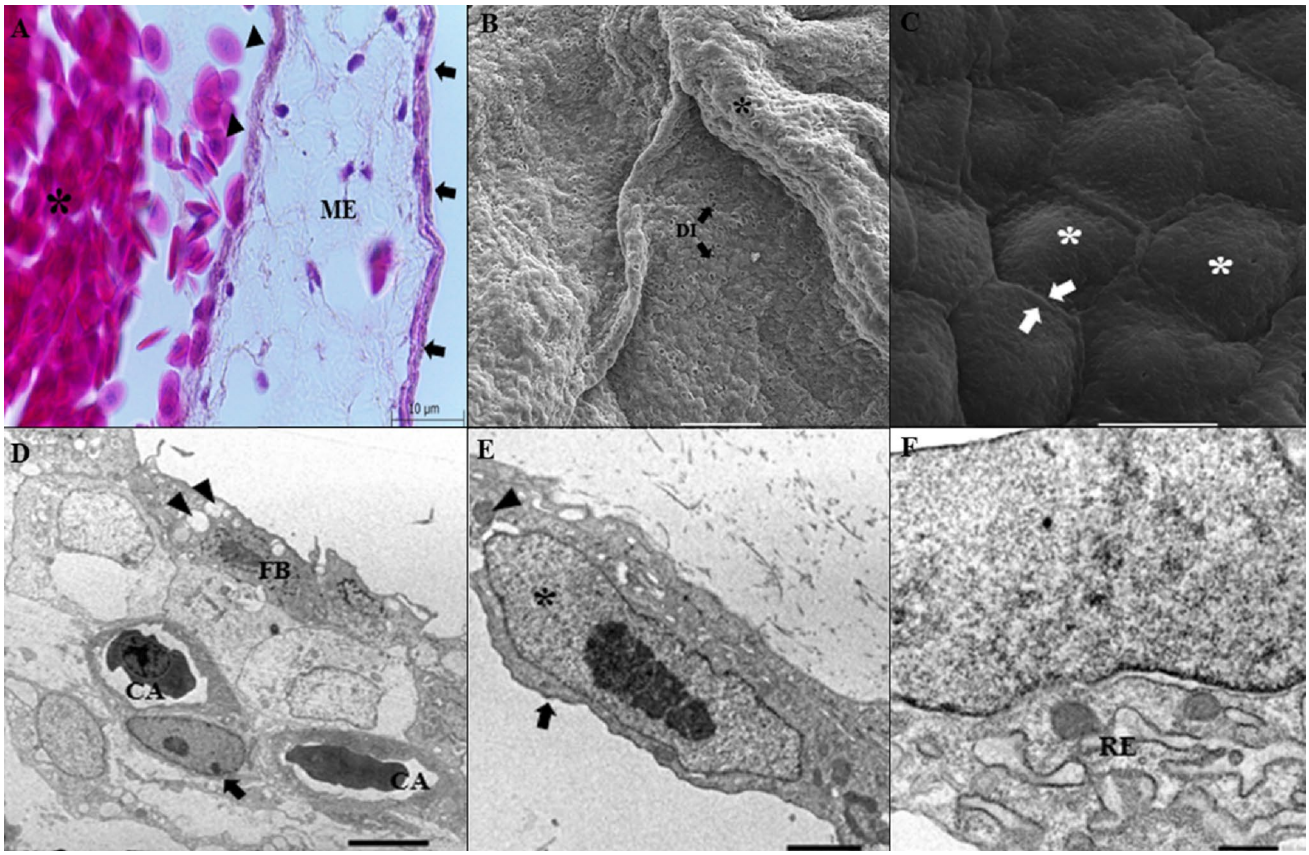

Fig. 5 Greater rhea allantois. **A** Light microscopy at 24 days of incubation, black arrow: ectoderm, black arrowhead: endoderm, *: blood vessels, *ME* mesoderm. **B** Scanning electron microscopy at 18 days of incubation, *DI* intervessel distances, *black (artery). **C** Scanning electron microscopy at 18 days of incubation, *white (endodermal epithelial cells), white arrows: cell boundaries. **D** Transmission electron microscopy at 18 days of incubation, *FB* fibroblast, black arrowhead: glycogen granules, *CA* blood capillary, arrow: pericyte. **E** Transmission electron microscopy at 18 days of incubation, black arrow: microvilli, *black: fibroblast, black arrowhead: glycogen granules. **F** Transmission electron microscopy at 18 days of incubation, *RE* rough endoplasmic reticulum. Bar: 10 µm, 100 µm, 10 µm, 5 µm, 2 µm, 500 nm

its very early development, as well as the presence of the allantoid and chorioallantoid membrane, which expand as a vascular network, providing gas exchanges and nutrient absorption increments to the developing embryo. These features concerning yolk sac appearance have also been reported by Saraswati and Tana (2015) for quails, by Hamburger and Hamilton (1951) for chickens and by Hanson (1954) for ducks. This sequential membrane development pattern is noted among several embryonic bird appendages, indicating phylogenetic aspect maintenance during ontogenesis (Saraswati and Tana 2015; Hanson 1954). The onset of extraembryonic membranes during early development also indicates that these structures comprise additional egg protection.

As soon as the extraembryonic membranes of greater rheas are established, at the beginning of the incubation period, their interaction degree is minimal, similarly to the vascular network that develops over these structures. Other authors have reported similar results for other species and observed an expansion between the extraembryonic membranes with time, such as Hamburger and Hamilton (1951) for chickens (*Gallus gallus domesticus*), Hanson (1954) for ducks (*Amas platyrhynchos* and *Ai sponsa*), Saraswati and Tana (2015) for quail (*Coturnix coturnix*) and Deeming (1995) for ostriches (*Struthio camelus*). These results indicate that avian embryo requirements in general, increase over time, not only in *Rhea americana*, so the embryos may grow and survive in eggs.

Divergences were observed concerning the appearance of embryonic annexes in greater rheas compared to other birds. For example, in chickens, the amnion emerges in 42 h, the chorion in 72 h and the chorioallantoid, after 5 days (Hamburger and Hamilton 1951), while in ducks, the amnion appeared after 5 days of incubation and the chorioallantoid, between the 8th and 11th day of incubation (Hanson 1954). In quails, the yolk sac is visible after 2 days, while the amnion and the allantoid appear on the 5th day and the chorioallantoid, by the 13th day, with quail

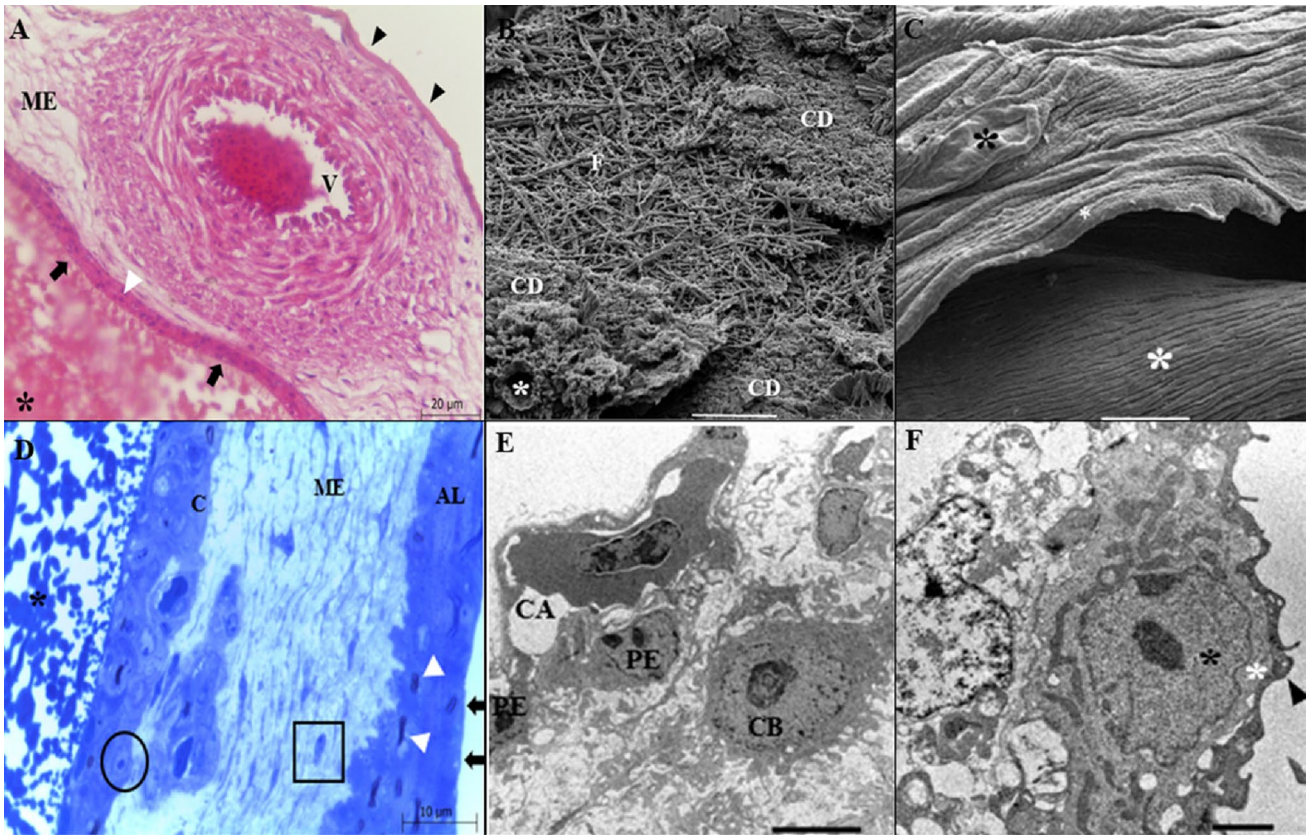

Fig. 6 Greater rhea chorioallantois + chorion + shell membrane at different ages. **A** Chorioallantois + shell membrane of rheas at 39 days of incubation, *black: fibers from the shell membrane, V: (blood vessels), ME: mesoderm, black arrow: ectoderm, white arrowhead: ectodermal cells, black arrowhead: endoderm. **B** Chorioallantois + shell membrane at 39 days of incubation, containing collagen fibers (F), pores (*) and calcium deposits (DC). **C** Chorioallantois + shell membrane at 28 days of incubation: *black: blood vessels, *white: membrane of the shell with collagen fibers. **D** Transmission electron microscopy, semi-thin sections of the chorioallantoic membrane shell membrane at 39 days of incubation, * black (shell membrane), **C** chorionic area, black circle: chorionic epithelial cells, ME: mesenchyme, mesoderm, black square: fibroblasts, white arrowhead: subepithelial layer of the allantois, AL: allantoic area, white arrowhead: allantoic epithelial, black arrow: allantoic ectoderm. **E**: Transmission electron microscopy of the chorion at 18 days of incubation, *CA* blood capillary, *PE* pericytes, *CB* basal cell. **F** Transmission electron microscopy of the chorion at 18 days of incubation, epithelial trabecula, *black: covering cell, *white: basement membrane, black arrowhead: endothelial lining. Bar: 20 µm, 200 µm, 50 µm, 10 µm, 5 µm and 2 µm

chicks able to leave the egg on day 16 (Saraswati and Tana 2015). Finally, the chorioallantoid membrane can be distinguished on the 21st day in ostriches (Deeming 1995). These differences are directly related to the incubation time of the species and associated to interspecific variations. Hotker (1998) reports that incubation temperatures, predation rates and the requirement for advanced development at hatching affect avian incubation period and embryonic development duration, which may also explain interspecies differences. Other groups, such as fish, reptiles and mammals, present different evolutionarily extraembryonic membrane development patterns, *i.e.,* fish exhibit only a yolk sac (Godinho and Godinho 2003), while reptiles display a yolk sac, amnion, chorion and allantois, similar to birds (Meneghel 2008). Mammals, however, display a placenta, yolk sac, amnion, allantois, chorion, and umbilical cord. This, in turn, leads to a lower degree of importance of the aforementioned appendages compared to birds, in which the yolk sac plays a truly trophic role until hatching, unlike is most mammals, where the yolk sac involutes as soon as the placenta develops (Garcia and Fernandes 2012).

When analyzing the role of these membranes as a whole, it becomes clear that the evolutionary process of each structure has acquired intrinsic functions associated with substance transport, vascularization, and embryo protection, and that they do not exhibit any particularities. Thus, the interrelation degree established by the juxtaposition between the amnion and allantoid, allantoid and chorion and the allantoid and yolk sac evolves or involutes, depending on the greater or lesser need for these membranes to fulfill their morpho-functional role. This is evidenced, for example, concerning the formation of the chorioallantoid membrane on the 12th

day of incubation in greater rheas, 5 days of incubation in *Gallus gallus domesticus* (Hamburger and Hamilton 1951), 21 days of incubation in *Struthio camelus* (Deeming 1995) and 13 days of incubation in *Coturnix coturnix japonica* (Saraswat and Tana 2015), where the embryos require greater nutrient supplies or substance transport at different developmental stages, even in greater rheas and ostriches, both ratites. Moreover, extrapolating to mammals, these would be the effective moments in which a chorioallantoid placenta would be performing its true function of substance transport and embryo protection. This, thus, demonstrates that the placenta is the most evolved structure among fetal annexes resulting from the interaction of more primitive structures, and that it is not formed in birds due to the lack of a key element, the mother's uterine environment, present in mammals. However, even though its participation in placenta formation may vary, it will always contribute to the ontogenic process (Oliveira 2004; Favaron 2015).

Microscopy analyses

Yolk sac

The light microscopy analyses concerning the yolk sac in greater rhea evidenced the presence of erythrocytes and cells originating from germinative leaflets, squamous in the ectoderm and large and prismatic in the endoderm. The presence of erythrocytes in the yolk sac can be associated to hematopoiesis, as previously discussed by Riveros et al. (2010). This feature been employed in the development of stem cell research (Riveros et al. 2010) and in understanding hematopoietic events in mammals (Guedes et al. 2014). Concerning germ cells, Sheng (2010) indicates erythrocytes in the yolk case during the earliest stages of chicken development, potentially associated to the formation and functioning of the primitive streak, as a relationship between these structures has been previously reported (Spratt and Haas 1965).

Concerning epithelial composition, Mobbs and Mcmillan (1981) state that greater rhea endoderm is composed of a simple, squamous epithelium. In *Coturnix coturnix japonica*, however, Starck (2020) cites that the yolk sac ectoderm consists in a simple squamous epithelium and that the endoderm is composed of a multiple-layer epithelium with large and prismatic cells directed towards the yolk. These findings demonstrate that yolk membrane constitutional structure and shape similarities between different birds are common, seemingly much more a result of interpretation than of morphological variations within this group.

The SEM analyses of vitelline endodermal cells indicated a rounded shape. Birds are not widely studied in this regard, and SEM assessments concerning the same structures have been reported only for reptiles, specifically the common kingsnake *Lampropeltis getula* by Kim and Blackburn (2015) and the pond slider *Trachemys scripta*, a semi-aquatic turtle, by Blackburn et al. (2019). Both studies report that these cells exhibit numerous rounded protuberances and commonly maintain contact with acellularized yolk sac areas. Their functionality according to Blackburn (2020) is to secrete enzymes into the yolk sac cavity and absorb extracellular digestion products, directly associated to one of the main avian yolk sac functions, which is to supply nutrients to developing embryos (Gadelha et al. 2021). We emphasize that the activity of this membrane in mammals is transient, as it loses its functionality soon after placenta formation in most animals (Oliveira 2004), unlike in birds and reptiles, where the yolk sac remains active until hatching, indicating a highly specialized membrane (Stewart and Blackburn 1988; Starck 2020).

We identified many mitochondria and a well-developed rough endoplasmic reticulum in greater rhea yolk sacs, as well as typical nucleoli and many lipid droplets, suggesting that these cells nourish the embryo. This corroborates other authors, who argue that these structures are associated with yolk trapping for subsequent embryo absorption, and the fact that lipid droplets have been similarly observed in chickens (Bellairs 1963; Lambson 1970). Furthermore, the shape of the endodermal and ectodermal cells found in greater rhea displays the same profile as in chickens (Bellairs 1963), indicating that these species share similar characteristics when it comes to extraembryonic membranes as analyzed by TEM.

Amnion

Greater rhea amnion displays an ectoderm constituted by stratified epithelium presenting cubic or columnar cells and an endoderm comprising paved epithelium containing a double layer of cubic cells, while the mesoderm is represented by loose connective tissue. The same characteristics in terms of epithelium and cell shape have been discussed for *Gallus gallus domesticus* by Davidson (1977), as well as the presence of a band of elongated ectoderm cells with a thick border in greater rhea, termed an amniotic crest by the Davidson (1977). This feature may be associated with the amniotic origin in birds, described as ectodermal by Vanderley and Santana (2015) and Monteiro (2017).

Amnion emergence allowed vertebrates the possibility of entering the terrestrial compartment, as it ensures embryonic development away from the aquatic environment. It also increases the chances of egg survival, guaranteeing a higher level of or extended protection (Rosslenbroich 2014), as it represents an aquatic reservoir that prevents the dehydration of the developing embryo, associated with the presence of a shell, highlighting its importance in ontogenic events. However, despite representing a key embryonic development structure in birds, little has been reported on avian extraembryonic membranes.

In addition, no articles describing bird amnion by SEM analyses are available, so our results are compared to human (Holbrook and Odland 1980) and sheep (Kaviani et al. 2001 and Kaviani et al. 2003) studies. Although these authors did not specify that the amnion presents polygonal cells, the available images in published articles are characteristic of polygonal structures.

We observed the presence of lipid droplets, microfilaments, and glycogen granules in the amnion membrane through the TEM analyses, similarly to features described in *Gallus gallus domesticus* (Davidson 1977). However, no studies reference amnion epithelium cells. The presence of lipid droplets may be associated to the amniotic transport pathway, which has been linked to the transport of certain nutrients, such as albumen proteins for later yolk absorption (Yoshizaki et al. 2002), although further studies are required to understand the presence of lipid droplets in the amniotic cavity.

Furthermore, ectodermal amnion cells are fibroblast-like, similar to the allantois, while endodermal border cells contain microvilli. In addition, numerous structures corresponding to collagen fibers were also visualized in the mesoderm. A high number of fibroblast cells in the amnion gives this structure the ability to expand as the embryo grows and becomes a fetus. Baggott (2009), in fact, refers to the amnion as a contractile membrane in a study on extraembryonic membrane development. Fibroblast cells have also been identified in human amnion by TEM assessments by Groothuis et al. (1998), exhibiting a similar conformation to that reported herein, comprising layers of compact connective tissue, fibroblasts, and loose connective tissue.

Despite the difficulties encountered in describing the amnion in greater rheas based on other birds, concerning the differentiation potential of epithelial stem cells, greater rheas cells exhibit multipotent stem cell characteristics when compared to chickens (Gao et al. 2012) and may, therefore, be used in tissue engineering and clinical studies, due to the presence of pluripotent and mesenchymal stem cells (Gadelha et al. 2021). Fetal fibroblasts from the amnion of other animals have been used in this regard (Yadav and Gulati 2013), also observed herein in the amnion of greater rheas, which may comprise a clinical alternative for the production of stem cells, as a large amount of these cells were detected.

Allantoid

The light microscopy allantois assessment in greater rhea indicated that the ectoderm is formed by multiple layers of cubic cells, while the mesoderm is composed of loose connective tissue, and the endoderm, of simple sidewalk cells. This is similar to that reported for chickens by Rangan and Sirsat (1962), Valdes et al. (2002) and Makanya et al. (2016), who indicate that the allantois is involved in cell aggregation through subepithelial mesoderm portions. Because of this, an increasing number of cells in this layer is noted over time, possibly associated to the chorioallantoid formation, as the mesenchyme and the allantoic epithelium alongside the chorionic epithelium are responsible for forming the chorioallantoid membrane (Makanya et al. 2016), and their aggregation was visible in the present study.

In general, studies involving the bird allantois employing SEM assessments analyze the allantois together with the chorionic membrane. We, however, analyzed this structure individually and in association with the chorion. The results of other studies for greater rhea indicate venules and arteries and the visualization of the capillary plexus and endodermal cells. The allantois is mostly studied alongside the chorion as even in the face of a single membrane, it is easily observed individually due to its abundance and capillary density, as indicated by Kim and Blackburn (2015) when researching fetal appendages in reptiles.

The SEM assessment carried out herein indicated capillary plexuses, intervascular distance, and differentiation between venules and arteries in the allantois of 12- and 18-day-old greater rheas, similar to those described in chickens and reptiles by Djonov et al. (2000), who reported a network of large capillaries which they indicate as having the function of supplying the short branches of this structure, and by Ribatti et al. (2001) when referring to a structure containing a capillary plexus and layers of supply vessels. According to Ferner and Mess (2011), blood capillaries are incorporated into the chorionic endothelium to form the chorioallantoid membrane with allantoid vascular system development. This expansion leading to chorioallantoic membrane formation allows the embryo to breathe, and the literature reports that the ability of the allantois to expand also allows for increased nutrient absorption in birds (Silva et al. 2017).

In birds, the formation of this membrane does not result in a placenta, but constitutes a link connecting the embryo to a vascular system, in close analogy to the functionality of the fetoplacental circulation observed in mammals, as described by Oliveira (2004) when referring to the chorioallantoid membrane as a juxtaposition of membranes that give rise to the placenta in order to establish embryonic circulation.

Kim and Blackburn (2015) observed flattened endodermal cells in *Lampropeltis getula*. The images in that paper also indicate a polygonal aspect, acquired during the development of the allantoid vessels, similar as to what is noted herein. According to the same authors, these cells acquire this appearance in mid-development, similar in shape to cells found on the chorionic surface. However, despite these findings, the functionality of these cells has not yet been described in the literature.

The TEM assessment of the allantois at 18 days of incubation indicated several fibroblasts and granules suggestive of the presence of glycogen, as well as blood capillaries, pericytes, intercellular junctions, erythrocytes, and lucent vesicles. Other authors reported similar results for chickens and in ducks, such as Makanya et al. (2016), who visualized fibroblasts extending into the mesenchyme, as well as microvilli and glycogen granules present in the outermost layer of the allantoid of chickens, and Lusimbo et al. (2000), who reported the presence of blood capillaries near the mesoderm and a well-developed rough endoplasmic reticulum in the allantoid epithelium in ducks, although they mention the existence of pericytes only in the chorionic epithelium. The presence of blood vessels and erythrocytes in the allantois is directly associated to the known functions this structure performs in avian embryos, such as vascularization for embryo expansion, chorioallantoid membrane formation and gas exchanges and calcium absorption, although the presence of glycogen granules may also be associated with the production of glycogen synthase kinase-3 (GSK-3) found only in avian embryos (Alon et al. 2011) and described as an important neuronal signaling regulator.

As discussed previously, the chorioallantoic membrane, alone or alongside other structures, performs essential egg functions, some of which may still be unknown. This membrane has sometimes been applied as a model for virus isolation and identification in the production of bird vaccines (Abd El Hafez et al. 2021), as well as an in vivo estrogen synthesis model (GILL et al. 1983). Studies employing this membrane regarding other functions should be more thorough, due to the presence of certain compounds reported herein, such as the glycogen granules found in the allantois, which may be associated with glycogen synthase kinase-3 related to bird signaling, cognition and neuronal behavior (Alon et al. 2011).

Chorioallantoid membrane + shell membrane

Regarding the chorioallantoid membrane, several studies have reported similar findings to those indicated in the present study, such as Lusimbo et al. (2000) regarding light microscopy assessments carried out in mallard ducks, in which elongated epithelial cells were observed in the allantoid epithelium and blood vessels in the mesoderm, and Yuan et al. (2014) in chickens, who demonstrated that this membrane consists of three layers, the first comprising chorionic epithelium, the second, allantoid epithelium and the third, an intermediate mesoderm termed the intermediate mesodermal layer, which lays between the chorionic and allantoid epithelium. The high amount of blood vessels found in greater rhea may lead to the use of the chorioallantoic membrane in diverse research, similarly to that of chickens, which has been used to study the growth of implanted tissues (Woodruff and Goodpasture 1931) and in neurosurgical disease studies (Yuan et al. 2014). In fact, greater rhea lay larger eggs, so the amount of available material would also be higher.

The scanning microscopy of the chorioallantois fragments collected from the shell membrane of 39-day old greater rheas demonstrated collagen fibers and calcium deposits in the shell membrane region and a capillary plexus with a large arrangement of capillaries in the chorioallantois region. Regarding the shell membrane, Packard (1980) discussed the presence of calcium carbonate in *Chelydra serpentina* shell membranes, also visualizing a parallel arrangement of fibers followed by randomly arranged fibers, inferring that these fibers probably play a role in allowing the membrane to expand without interruption during ontogenetic development. The amount of calcium deposits in the shell membrane of greater rheas and the proximity of this membrane to the chorioallantoic membrane are indicative that the chorioallantoic membrane assists in bone formation by transporting calcium to the embryo, as previously described by Monteiro (2017).

As for the chorioallantoid membrane, Kim and Blackburn (2015) state that the chorionic and allantoid epithelia thin dramatically and become supported by a rich network of allantoid capillaries in reptiles (*Lampropeltis getula*), producing a membrane ideally suited for respiratory gas exchanges. This thinning was also noticed herein throughout the developmental period, where the more advanced the development stage, the more easily the membranes are ruptured and the more expressive is the number of vessels that compose the vascular network. Another aspect to consider regarding the proximity of the chorioallantoid and shell membrane is that one of its final functions is to guarantee gas exchanges required for embryo maintenance. This need increases throughout the incubation process to the point that it juxtaposes with the innermost surface of the shell membrane. Ferner and Mess (2011) infer that the proximity observed between the shell membrane and the chorioallantois is directly associated to O_2 and CO_2 gas exchanges in avian embryos, and that this, in turn, depends on shell membrane diffusion and cardiovascular convection via the chorioallantoid membrane.

The semi-thin section analyses carried out herein indicated oval epithelial cells in the chorionic portion of greater rhea fetuses at 39 days of incubation, as well as elongated epithelial cells in the allantoid constitution, in addition to blood vessels and evenly distributed cells in the mesoderm (structure mesenchyme). Makanya et al. (2016) also observed mesenchymal uniformity in the same structure in chickens and reported that the contour of the epithelial layers in both cases (allantoid layer and chorionic layer) are irregular. These epithelial cells are also found in chickens, along with immature blood vessels that comprise important gas

exchange mediators with the external environment (Ribatti et al. 2001).

Concerning the TEM analyses, some authors have reported similar results for tapirs, such as the presence of pericytes, epithelial trabeculae, capillaries, and a chorionic epithelium with basal cells. These findings were also described by Hoshi and Mori (1971) when studying the structure of the chorionic epithelium of chickens, who indicated cover cells arranged under the basal cell layer, similar to that reported herein. These cover cells form trabeculae that traverse the layer of sinusoidal capillaries, which contain pericytes-like nerve structures. Similar results were also reported for ducks by Lusimbo et al. (2000) and for chickens by Makanya et al. (2016). The presence of blood capillaries indicates that, as noted for chickens (Ribatti et al. 2001), the chorioallantoid of greater rheas can also be employed as an in vivo model for angiogenesis and antiangiogenesis studies.

In addition, the chorioallantoic membrane of greater rheas may also be employed in other fields, as noted for smaller birds, such as in the evaluation of toxicological effects (Oliveira et al. 2012), in determining vascular responses and in understanding issues related to blood vessel and lymphatic morphogenesis and physiology (Nowak-Sliwinska et al. 2014).

Extraembryonic membrane evolutionary process

Ferner and Mess (2011), in a review addressing embryonic annex evolution, mention that these annexes evolved to harmonize certain ontogenic process restrictions in different animal groups, such as gross size, habitat and life habits, and that, as a result, the placenta did not evolve linearly, which would seem ideal, leading different taxa to find different solutions to guarantee the necessary metabolic exchanges for their fetuses. Carter (2012) states that all fetal attachments contribute to placenta formation, further emphasizing the importance of this evolutionary process, also highlighting that a placenta is formed from the yolk sac at a critical stage of embryo development in many mammals, allowing the embryo to survive until the allantois expands and juxtaposes to the chorion, giving rise to the chorioallantoid placenta, with functions supported by genes evolved from common ancestors. Thus, fetal attachment development in greater rheas and the very well-founded understanding on this subject both point to ancestral yolk sac characteristics, a structure primitively passed on to different vertebrate taxa, which alongside the amnion, allantois and chorion, assume very similar functions in the ontogenic processes of different animal groups. This may, in turn, result in the development of a placenta whose specialization would be associated with the fetal requirements within each taxon and that translates into genetic information passed on from individual to individual throughout evolutionary processes and natural selection.

The presence of distinct layers in the germinal leaflets of the ectoderm, mesoderm, and endoderm in greater rheas is also an indication that fetal appendages have not suffered evolutionarily significant morphological modifications over the time. Furthermore, the chorionic membrane presents itself as vascularized in birds such as greater rhea, chickens and ducks and is an avascular structure in mammals, representing the loss of an evolutionary feature over time, replaced by the development of a placenta in groups higher up the evolutionary scale, such as mammals.

Conclusions

The fact that the amnion, allantois, yolk sac, and chorion exhibit a vascular network throughout greater rhea embryonic development indicates that they share the same purposes in the embryo development process, including nutrient, gas, water, and calcium transport, as well as nitrogenous excreta, among others.

Greater rhea extraembryonic membrane characteristics, such as the presence of erythrocytes in the yolk sac, fibroblastic cells in the amnion and allantois, glycogen granules and a high amount of blood capillaries in the chorioallantoic membrane, allow the extraembryonic membranes of these animals to be used as a clinical and scientific model for obtaining stem cells, and as in proteomics and cell therapy studies, as well as in toxicological evaluations and vaccine development.

Furthermore, greater rheas are highly adaptable to captive breeding and lays large eggs. Despite the development pattern observed in these animals in terms of cellular constitution, number of membrane layers and similar morphological vascularization features to other avians, we infer that this animal may comprise an excellent model for the development of extraembryonic annex research.

Acknowledgements The authors would like to thank the Coordination for the Improvement of Higher Education Personnel (CAPES, Financial Code 001) for the master's degree scholarship granted to the Postgraduate Program in Animal Science (PPGCA-UFERSA).

Author contributions AIBBG: wrote the main manuscript text, MFdO: developed the methodology and did the data validation, ACFCdS: worked on the data collection, JARAD and IRGL: worked on data analysis, BCCF: handled the softwares, AFP and CEBdM: worked on literature review.

Data availability All data used in this study are available upon personal request to the authors.

Declarations

Conflict of interest The authors declare that they have no conflict of interest.

Consent to participate Not applicable.

Consent for publication Authors declare that they know the content of this manuscript and agreed to submit it to Zoomorphology.

References

Abd El Hafez MS, Shosha EM, Ibrahim SM (2021) Isolation and molecular detection of pigeon pox virus in Assiut and New Valley governorates. Journal of Virological Methods 293:114142. https://doi.org/10.1016/j.jviromet.2021.114142

Almeida MH, Sousa PR, Bezerra OD, Olivindo GFR, Diniz NA, Oliveira CS, Feitosa TLM, Fortes MAE, Ferraz SM, Carvalho PKY, Menezes AJD, Carvalho MAM (2015) Greater rhea (Rhea americana) external morphology at different stages of embryonic and fetal development. Animal Reproduction Science 162:43–51. https://doi.org/10.1016/j.anireprosci.2015.09.007

Alon LT, Pietrokovski S, Barkan S, Avrahami L, Kaidanovich-Beilin O, Woodgett JR, Barnea A, Eldar-Finkelman H (2011) Selective loss of glycogen synthase kinase-3α in birds reveals distinct roles for GSK-3 isozymes in tau phosphorylation. Febs Lett 585(8):1158–1162. https://doi.org/10.1016/j.febslet.2011.03.025

Baggott GK (2009) Development of extra-embryonic membranes and fluid compartments. Avian Biol Research 2:21–26. https://doi.org/10.3184/175815509X43038

Bellairs R (1963) Differentiation of the yolk sac of the chick studied by electron microscopy. J Embryol Exp Morphol 11:201–225. https://doi.org/10.1242/dev.11.1.201

Blackburn DG (2020) Functional morphology, diversity, and evolution of yolk processing specializations in embryonic reptiles and birds. J Morphol 282(7):995–1014. https://doi.org/10.1002/jmor.21267

Blackburn DG, Lestz LL, Barnes MS, Appiah FA, Bonneau LJ (2019) Ultrastructural analysis of the yolk processing pattern in embryonic pond slider turtles (*Trachemys scripta*: Emydidae). J Exp Zool B Mol Dev Evol 332(6):187–197. https://doi.org/10.1002/jez.b.22894

Carter MA (2012) Evolution of placental function in mammals: the molecular basis of gas and nutrient transfer, hormone secretion, and immune responses. Physiol Rev 92:1543–1576. https://doi.org/10.1152/physrev.00040.2011

Costa HS, Araújo JHN, Bezerra FVF, Rebouças CE, Menezes DJA, Moura CEB, Oliveira MF (2018) Macroscopic anatomy and brain vascularization in the Greater Rhea (*Rhea americana americana*). Acta Sci Vet 46:8. https://doi.org/10.22456/1679-9216.86671

Davidson FI (1977) Um estudo descritivo e experimental da formação de dobra amniótica no embrião de frango. Dissertation, The University of Texas at Austin.

Deeming DC (1995) The hatching sequence of ostrich (*Struthio camelus*) embryos with notes on development as observed by candling. Br Poult Sci 36(1):67–78. https://doi.org/10.1080/00071669508417753

Djonov V, Schmid M, Tschanz SA, Burri PH (2000) Intussusceptive angiogenesis: its role in embryonic vascular network formation. Circulation research 86(3):286–292. https://doi.org/10.1161/01.RES.86.3.286

Favaron PO, Carvalho RC, Borghesi J, Anunciação ARA, Miglino MA (2015) The amniotic membrane: development and potential applications–a review. Reprod Domest Anim 50(6):881–892. https://doi.org/10.1111/rda.12633

Ferner K, Mess A (2011) Evolution and development of fetal membranes and placentation in amniote vertebrates. Respir Physiol Neurobiol 178:39–50. https://doi.org/10.1016/j.resp.2011.03.029

Gadelha AIBB, Sousa ACFC, Diniz JARA, Moura CEB, Assis Neto AC, Oliveira MF (2021) Os anexos embrionários de aves: revisão de literatura. Res Soc Dev 10(2):1–10. https://doi.org/10.33448/rsd-v10i2.12498

Gao Y, Pu Y, Wang D, Zhang W, Guan W, Ma Y (2012) Isolation and biological characterization of chicken amnion epithelial cells. Eur J Histochem 56(3):33. https://doi.org/10.4081/ejh.2012.e33

Garcia LMS, Fernández GC (2012) Embriologia. Artmed Editora LTDA, Porto Alegre

Gill DV, Robertson HA, Betz TW (1983) In vivo estrogen synthesis by the developing chicken (Gallus gallus) embryo. General and Comparative Endocrinology 49(2):176–186. https://doi.org/10.1016/0016-6480(83)90134-X

Godinho HP, Godinho AL (2003) São Francisco das Minas Gerais. Editora Pucminas, Belo Horizonte MG

Groff PM, Takahashi SE, Padilha JB, Bochio V, Schadeck MM, Maier GS, Gorges MH, Santos IL, Emilyn MM (2017) Importance of temperature and humidity and the effects of light during incubation offer tile eggs of chickens. Redvet 18(2):021–707

Groothuis PG, Koks CA, Goejj AF, Dunselman GA, Arends JW, Ever JL (1998) Adhesion of human endometrium to the epithelial lining and extracellular matrix of amnion in vitro: an electron microscopic study. Human Reproduction (oxford, Inglaterra) 13(8):2275–2281. https://doi.org/10.1093/humrep/13.8.2275

Guedes PT, Abreu MPP, Caputo LFG, Cotta-Pereira G, Pelajo MM (2014) Histological analyses demonstrate the temporary contribution of yolk sac, liver, and bone marrow to hematopoiesis during chicken development. PLoS One 9(3):1–8. https://doi.org/10.1371/journal.pone.0090975

Hamburger V, Hamilton HL (1951) A series of normal stages in the development of the chick embryo. J Morphol 88(1):49–92

Hanson HC (1954) Criteria of age of incubated mallard, wood duck, and bob-white quail eggs. Auk 71(3):267–272. https://doi.org/10.2307/4081668

Holbrook KA, Odland GF (1980) Regional development of the human epidermis in the first trimester embryo and the second trimester fetus (ages related to the timing of amniocentesis and fetal biopsy). J Investig Dermatol 74(3):161–168. https://doi.org/10.1111/1523-1747.ep12535062

Hoshi H, Mori T (1971) The fine structure of the chorionic epithelium of chick embryos. Arch Histol Jap 33:45–58. https://doi.org/10.1679/aohc1950.33.45

Hotker HE (1998) Intraspecific variation in length of incubation period in Avocets Recurvirostra avosetta. Ardea-Wageningen 86:33–42

Kaviani A, Perry TE, Dzakovic A, Jennings RW, Ziegler MM, Fauza DO (2001) The amniotic fluid as a source of cells for fetal tissue engineering. J Pediatr Surg 36(11):1662–1665. https://doi.org/10.1053/jpsu.2001.27945

Kaviani A, Guleserian K, Jennings RW, Ziegler MM, Fauza DO (2003) Fetal tissue engineering from amniotic fluid. J Am Coll Surg 196(4):592–597. https://doi.org/10.1016/S1072-7515(02)01834-3

Kim YK, Blackburn DG (2015) Ultrastructure of the fetal membranes of the oviparous kingsnake, *Lampropeltis getula* (Colubridae) as revealed by scanning electron microscopy. J Morphol 276(12):1467–1481. https://doi.org/10.1002/jmor.20435

Lambson RO (1970) An electron microscopic study of the endodermal cells of the yolk sac of the chick during incubation and after hatching. Am J Anat 129(1):1–19. https://doi.org/10.1002/aja.1001290102

Lusimbo SW, Leighton AF, Wobeser AG (2000) Histology and ultrastructure of the chorioallantoic membrane of the mallard duck

(*Anas platyrhynchos*). Anat Rec 259:25–34. https://doi.org/10.1002/(SICI)1097-0185(20000501)259:1%3C25::AID-AR3%3E3.0.CO;2-Y
Makanya AN, Dimova I, Koller T, Styp-rekowska B, Djonov V (2016) Dynamics of the developing chick chorioallantoid membrane assessed by stereology, allometry, immunohistochemistry and molecular analysis. PLoS One 11(4):1–23. https://doi.org/10.1371/journal.pone.0152821
Meneghel M (2008) Clase Reptilia. Recuperado El 8:1–19
Mess A (2003) Evolutionary transformations of chorioallantoid placental characters in Rodentia with special reference to hystricognath species. J Exp Zool A Comp Exp Biol 299:78–98. https://doi.org/10.1002/jez.a.10292
Mobbs IG, Mcmillan DB (1981) Transport across endodermal cells of the chick yolk sac during early stages of development. Am J Anat 160(3):285–308. https://doi.org/10.1002/aja.1001600307
Monteiro AP (2017) Histologia e embriologia comparada. Editora e Distribuidora Educacional S.A., Londrina
Narbaitz R, Bastani B, Galvin NJ, Kapal VK, Levine DZ (1995) Ultrastructural and immunocytochemical evidence for the presence of polarised plasma membrane H (+)-ATPase in two specialised cell types in the chick embryo chorioallantoid membrane. J Anat 186:245
Nowak-Sliwinska P, Segura T, Iruela-Arispe ML (2014) The chicken chorioallantoic membrane model in biology, medicine and bioengineering. Angiogenesis 17(4):779–804. https://doi.org/10.1007/s10456-014-9440-7
Oliveira MFD (2004) Placentação em mocós, *Kerodon rupestris* Wied, 1820. Doctoral dissertation, Universidade de São Paulo
Oliveira AGL, Silva RS, Alves EN, Farias PR, Presgrave OAF, Delgado IF (2012) Ensaios da membrana cório-alantoide (HET-CAM e CAM-TBS): alternativas para a avaliação toxicológica de produtos com baixo potencial de irritação ocular. Rev Inst Adolfo Lutz 71(1):153–159
Ouyang JQ, Quetting M, Hau M (2012) Corticosterone and brood abandonment in a passerine bird. Anim Behav 84:261–268. https://doi.org/10.1016/j.anbehav.2012.05.006
Packard MJ (1980) Ultrastructural morphology of the shell and shell membrane of eggs of common snapping turtles (*Chelydra serpentina*). J Morphol 165(2):187–204. https://doi.org/10.1002/jmor.1051650207
Rangan SRS, Sirsat SM (1962) The fine structure of the normal chorioallantoic membrane of the chick-embryo. J Cell Sci 3(61):17–23
Ribatti D (2012) Chicken chorioallantoid membrane angiogenesis model. Cardiovascular development, vol 843. Humana Press, pp 47–57. https://doi.org/10.1007/978-1-61779-523-7_5
Ribatti D, Nico B, Vacca A, Roncalli L, Burri PH, Djonov V (2001) Chorioallantoid membrane capillary bed: a useful target for studying angiogenesis and anti-angiogenesis in vivo. Anat Rec off Publ Am Assoc Anat 264(4):317–324. https://doi.org/10.1002/ar.10021
Riveros GCA, Rezende CL, Pessolato TGA, Miglino AMA (2010) Relação Biológica Entre o Saco Vitelino e o Embrião. Enciclopédia Biosfera 6:1–8
Romanelli FP, Trabuco E, Scriboni BA, Visentainer VJ, Souza EN (2008) Chemical composition and fatty acid profile of rhea (*Rhea americana*) meat. Arch Latinoam Nutr 58(2):201–205
Rosslenbroich B (2014) Reproduction. On the origin of autonomy history philosophy and theory of the life sciences. Springer Science & Business Media, New York
Saraswati TR, Tana A (2015) Development of Japanese quail (Coturnix coturnix japonica) embryo. International Journal of Science and Engineering 8(1):3841. https://doi.org/10.12777/ijse.8.1.38-41
Sheng G (2010) Primitive and definitive erythropoiesis in the yolk sac: a bird's eye view. Int J Dev Biol 54:1033–1043. https://doi.org/10.1387/ijdb.103105gs
Sick H (2001) Ornitologia brasileira. Editora Nova Fronteira, Rio de Janeiro
Silva M, Labas V, Nys Y, Réhault-Godbert S (2017) Investigating proteins and proteases composing amniotic and allantoic fluids during chicken embryonic development. Poultry science 96(8):2931–2941. https://doi.org/10.3382/ps/pex058
Sousa RP, Monteiro HMDA, Bezerra DDO, Soares LLDS, Assis Neto AC, Rici RE, Junior CMA, Carvalho MA (2018) Morphogenesis of the rhea (*Rhea americana*) respiratory system in different embryonic and foetal stages. Pesq Vet Bras 38:154–166. https://doi.org/10.1590/1678-5150-PVB-5310
Spratt NTJR, Haas H (1965) Germ layer formation and the role of the primitive streak in the chick. I. basic architecture and morphogenetic tissue movements. J Exp Zool 158:9–38
Starck JM (2020) Morphology of the avian yolk sac. J Morphol 282(7):959–972. https://doi.org/10.1002/jmor.21262
Stewart JR, Blackburn DG (1988) Reptilian placentation: structural diversity and terminology. Copeia 1988:838–851. https://doi.org/10.2307/1445706
Thierry MA, Couder RY, Raclot T (2013) Elevated corticosterone levels decrease reproductive output of chick-rearing Adélie penguins but do not affect chick mass at fledging. Conserv Physiol 1:1–12. https://doi.org/10.1093/conphys/cot007
Tolosa EMC, Rodrigues CJ, Behmer AO, Freitas Neto AG (2003) Manual de Técnicas para Histologia Normal e Patológica. Editora Manole Ltda, Barueri SP
Torquato JL, Sousa JBF, Queiroz JPAF, Costa LLM (2015) Termografia infravermelha aplicada a emas (*Rhea americana*). J Anim Behav Biometeorol 3:51–56. https://doi.org/10.14269/2318-1265/jabb.v3n2p51-56
Valdes TI, Kreutzer D, Moussy F (2002) The chick chorioallantoid membrane as a novel in vivo model for the testing of biomaterials. J Biomed Mater Res off J Soc Biomater Jpn Soc Biomater Aust Soc Biomater Korean Soc Biomater 62(2):273–282. https://doi.org/10.1002/jbm.10152
Vanderley SBSC, Santana HCI (2015) Histologia e Embriologia Animal Comparada. Editora UECE, Fortaleza CE
Vargas A, Zeisser-labouebe M, Lange N, Gurny R, Delie F (2007) The chick embryo and its chorioallantoid membrane (CAM) for the in vivo evaluation of drug delivery systems. Adv Drug Deliv Rev 59:1162–1176. https://doi.org/10.1016/j.addr.2007.04.019
Winter V, Elliot JE, Letcher RJ, Williams TD (2013) Validation of an egg-injection method for embryotoxicity studies in a small, model songbird, the zebra finch (*Taeniopygia guttata*). Chemosphere 90:125–131. https://doi.org/10.1016/j.chemosphere.2012.08.017
Woodruff AM, Goodpasture EW (1931) The susceptibility of the chorio-allantoic membrane of chick embryos to infection with the fowl-pox virus. Am J Pathol 7(3):209
Yadav PS, Gulati BR (2013) Fetal mesenchymal stem cells in farm animals: applications in health and production. In: Salar R, Gahlawat S, Siwach P, Duhan J (eds) Biotechnology prospects and applications. Springer, New Delhi
Yoshizaki N, Yasushi ITOY, Hori H, Saito H, Iwasawa A (2002) Absorption, transportation and digestion of egg white in quail embryos. Dev Growth Differ 44:11–22
YuanYJ XuK, Wu W, Luo Q, Yu JL (2014) Application of the chick embryo chorioallantoid membrane in neurosurgery disease. Int J Med Sci 11(12):1275. https://doi.org/10.7150/ijms.10443